

Modeling and Optimization of Arsenic (III) Removal from Aqueous Solutions by GFO Using Response Surface Methodology

Tabatabaei, F.S.¹, Izanloo, H.¹, Heidari, H.¹, Vaezi, N.¹, Zamanzadeh, M.², Nadali, A.³, Aali, R.¹ and Asadi-Ghalhari, M.^{1*}

1. Research Center for Environmental Pollutants, Qom University of Medical Sciences, Qom, Iran.
2. Department of Environmental Health Engineering, School of Public Health, Tehran University of Medical Sciences, Tehran, Iran
3. Department of Environmental Health Engineering, School of Public Health, Hamadan University of *Medical Science*, Hamadan, Iran

Received: 22.01.2020

Accepted: 27.05.2020

ABSTRACT: Arsenic is a highly toxic element for human beings, which is generally found in groundwater. Dissolved Arsenic in water can be seen as As^{+3} and As^{+5} states. The adsorption process is one of the available methods to remove Arsenic from aqueous solutions. Thus, this paper aims at removing Arsenic (III) from aqueous solutions through adsorption on iron oxide granules. The relation among four independent variables, namely the initial concentration of Arsenic (III), pH, adsorbent dose, and contact time have been investigated through Response Surface Methodology. Design-Expert software and Central Composite Design method have been used to design and analyze the experiments and results. Also, SEM and FTIR analysis have been conducted to characterize the adsorbent morphology. The optimum initial concentration of Arsenic (III), pH, contact time, and adsorbent dosage are 30ppm, 5, 49.99min, and 8g/l, respectively. Under these optimum conditions, the Arsenic (III) removal efficiency is 67%. The predicted 2FI model shows the highest Arsenic removal coefficient ($R^2=0.887$).

Keywords: Adsorption, Arsenic (III), Iron Oxide Granules (GFO), aqueous solutions.

INTRODUCTION

Arsenic is a highly toxic chemical element (Mao et al., 2019). Typically, this element can be found in the environment in several oxidation states (+5, +3, 0, and -3) (Litter, Morgada, & Bundschuh, 2010). In water, dissolved Arsenic can be seen as As^{+3} and As^{+5} states. At a pH range of 2-12, the latter (As^{+5}) could exist as $H_2AsO_4^-$ and $HAsO_4^{2-}$, whereas the former (As^{+3}) exists at a pH value below 9.2 and as $H_3AsO_3^0$ (Cheng, Fu, Dionysiou, & Tang, 2016; Salameh, B. Albadarin, Allen, Walker, & Ahmad, 2015). In underground water,

arsenic is more likely to be found as Arsenite, a more toxic, soluble, and fluidic variety than Arsenic (Cheng et al., 2016).

Arsenic is known as a carcinogen factor for human organs (Malakootian et al., 2018) such as skin, lung, kidneys (Nasir, Goh, & Ismail, 2018), and liver (Salameh et al., 2015). It is estimated that at least 150 million people around the world are exposed to arsenic contaminated water (Bhandari, Reeder, & Strongin, 2012). There are reports of high arsenic-contaminated water in many parts of the world, like Bangladesh (Gupta, Yunus, & Sankararamakrishnan, 2012), China (Bringas, Saiz, & Ortiz, 2015), Argentina (Guivar et al., 2018), North

* Corresponding Author, Email: mehdi.asady@gmail.com

America (Ociński, Jacukowicz-Sobala, Mazur, Raczyk, & Kociołek-Balawejder, 2016), Taiwan (Barati, Maleki, & Alasvand, 2010), Mexico (Pillewan et al., 2011), etc. Because of the hazardous effects of arsenic on human health, many countries are applying a maximum permissible limit of 10µg/L (recommended by the World Health Organization) for arsenic in drinking water (Wang, Xu, Chen, Huang, & Liu, 2014).

Technologies such as coagulation (AlOmar, Alsaadi, Hayyan, Akib, & Hashim, 2016), ion exchange, membrane filtration, adsorption (Jian, Liu, Zhang, Liu, & Zhang, 2015; Lata & Samadder, 2016), oxidation with ozone, and electrochemical are being used to remove arsenic from potable water (Chang, Lin, & Ying, 2010). Among the available methods, adsorption is the most reliable one, as it does not add any by-products and can be possibly regenerated for reuse (Lata & Samadder, 2016). However, it should be noticed that most adsorbents have a mineral base, making them quite expensive and, as a result, a less likely option for removal of arsenic (Nadali, Khoobi, Nabizadeh, Naseri, & Mahvi, 2016). Therefore, this study tries to produce iron oxide granules through an easy and inexpensive method (electrolysis) and use it as an adsorbent for arsenic. As mentioned before, arsenite is one of the toxic forms of arsenic. Hence the prespen paper mainly seeks to investigate the efficiency of granular ferric oxide (GFO) in removal of arsenic (III) from aqueous solutions. In addition, the paper attempts to enhance the performance of this adsorbent by considering the key factors of the process. As for the experiments, they have been optimized through Respond Surface Method (RSM), for it goes without saying that optimizing the process condition, reducing the operating costs, and the maximum removal efficiency are important issues (Lee, Krongchai, Lu, Kittiwachana, & Sim, 2015). RSM can predict different possible scenarios through a mathematical method. It shows the effect of

each factor independently, demonstrating the impact of each factor on independent variables (Usefi & Asadi-Ghalhari, 2019). Four independent variables, including the initial arsenic concentration, pH, GFO dose, and contact time are selected and evaluated at five levels (+α, +1, 0, -1, and +α). Design-Expert software, v. 7.0.0, has been used to design the experiments (Mostafaloo, Mahmoudian, & Asadi-Ghalhari, 2019).

MATERIALS AND METHODS

All chemical compounds were of analytical grade. Sodium Arsenite solution ($\text{NaAsO}_2=0.05\text{mol/L}$), NaCl, HCl, HNO_3 , and NaOH were purchased from Merck (Darmstadt, Germany). Arsenite stock solution was stored at 4°C in a refrigerator. The required solutions of Arsenite were prepared daily by diluting the stock solution with deionized water.

In this study, the adsorbent was prepared via electrochemical method (electrolysis). Sodium Bicarbonate solution and iron sheets were used as electrolyte and electrodes, respectively. The yielded dark color precipitate was washed several times by deionized water and then dried in an oven at 100°C for 2h. Afterwards, the dried adsorbent was ground and placed in a furnace at 600°C for 3h to convert iron oxide into GFO. After preparation, the adsorbent got stored in a desiccator and container for further use.

The functional groups of synthesized GFO were determined by means of Fourier Transform Infrared Spectroscopy (FTIR, Tensor 27 model, Bruker). After being ground into powder, the sample got mixed entirely with potassium bromide, thence to be pelleted by entering into a disk and getting scanned at wavelengths between 450 and 4000 cm^{-1} . The morphology of GFO was taken by the scanning electron microscope (SEM, HITACHI-4160 model).

Considering that many factors are effective on adsorption of arsenite on granular ferric oxide, the parameters were

optimized via Respond Surface Method (RSM), based on Central Composite Design (CCD). Design-Expert, v.7, was utilized to design and analyze the experiments and the results. In this design, four variables were defined at five levels. The influence of main factors on removal efficiency of Arsenic (III) by GFO was studied with the RSM method.

Table 1 illustrates the main factors and their levels. Table 2 demonstrates the matrix of experiments and their response through CCD. As it can be seen in Table 2, there were thirty experiments in total.

To evaluate the adsorption of Arsenic (III) on GFO, a batch reactor was used. Also, the pH value of the solution was adjusted with

1M NaOH or HNO₃. Nonetheless, the samples were centrifuged and filtered through a 0.45-micron membrane. Afterwards, the samples were poured into plastic containers and by adding concentrated HNO₃, their pH remained below 2. The ICP-MS instrument was used to determine the Arsenic (III) concentration of samples (Andrew, Eugene, & Lenore, 2005). Finally, the removal efficiency of Arsenic (III) on GFO was determined by Eq. (1).

$$R\% = \frac{C_0 - C_t}{C_0} \times 100 \tag{1}$$

where C₀ and C_t are the initial and final concentration of Arsenic (III) in the solution (mg/l), respectively.

Table 1. Coded and actual values and their levels

Variables	Symbol	Coded Variable level				
		1-	α-	0	α+	1+
Contact time (min)	X ₁	5	20	35	50	65
Adsorbent dose(g/L)	X ₂	2	4	6	8	10
Arsenite concentration(mg/L)	X ₃	10	30	50	70	90
pH	X ₄	3	5	7	9	11

Table 2. The matrix of the experiments with CCD design and coded factor levels for arsenite removal as well as the response value

Experimental run (n)	Experimental design					Removal efficiency	
	Time (min)	Dose (g/l)	Concentration (ppm)	pH	Actual value	Predicted value	
1	50	4	70	9	25.99	23.63	
2	50	4	70	5	18.45	21.79	
3	35	6	10	7	35.48	41.40	
4	35	6	50	3	37.22	40.16	
5	35	6	90	7	38.21	35.93	
6	65	6	50	7	41.51	40.64	
7	35	6	50	11	33.56	37.17	
8	20	8	70	9	44.31	45.77	
9	50	8	70	5	43.72	44.46	
10	20	4	30	9	28.47	29.04	
11	50	4	30	9	18.87	22.57	
12	35	6	50	7	38.37	38.66	
13	50	4	30	5	37.46	37.31	
14	20	4	70	9	43.86	46.12	
15	35	6	50	7	44.31	38.66	
16	35	6	50	7	43.72	38.66	
17	50	8	30	5	67.02	67.00	
18	20	8	30	5	36.89	40.56	
19	5	6	50	7	37.52	36.69	
20	20	8	70	5	35.48	34.03	
21	50	8	30	9	57.27	53.22	
22	35	6	50	7	36.99	38.66	
23	35	2	50	7	29.35	23.99	
24	35	6	50	7	42.39	38.66	
25	20	4	30	5	38.55	34.84	
26	50	8	70	9	41.29	47.25	
27	35	6	50	7	40.1	38.66	
28	20	8	30	9	36.81	35.72	
29	20	4	70	5	29.97	35.33	
30	35	10	50	7	56.8	53.34	

RESULTS AND DISCUSSION

GFO morphology was characterized by SEM analysis, using a HITACHI S-4160 microscope at an acceleration voltage of 30kV. The working distance was 5nm and the magnification ranged between 20 and 3000. Fig.1 presents the GFO images before and after adsorption. According to Fig.1-b, the granules of GFO became coarser and the absorbent surface was changed completely.

Studies reveal that the GFO is a combination of Iron Oxides with Fe_2O_3 70% (Kabay et al., 2010). Indeed, Iron Oxide granules belong to hematite with a structural formula of $\alpha\text{-Fe}_2\text{O}_3$ (Cornell & Schwertmann, 2003) that has a cubic or

elliptical structure and their color is bright red (Kabay et al., 2010).

FTIR spectra at a wavelength of 400-4000 cm^{-1} show the chemical bands of GFO (Fig.2). The analysis indicates that the band at 3445.3 cm^{-1} was related to the water. Furthermore, the peak at 1630 cm^{-1} was associated with the stretching and bending bands of water molecules. Similarly, the displayed band at about 550 cm^{-1} belonged to the vibration of Fe-O stretching in FeO_6 octagonal structure (Jiangying Wang et al., 2014). The band demonstrated at 471.5 can determine the $\alpha\text{-Fe}_2\text{O}_3$ (Ristić, De Grave, Musić, Popović, & Orehovec, 2007).

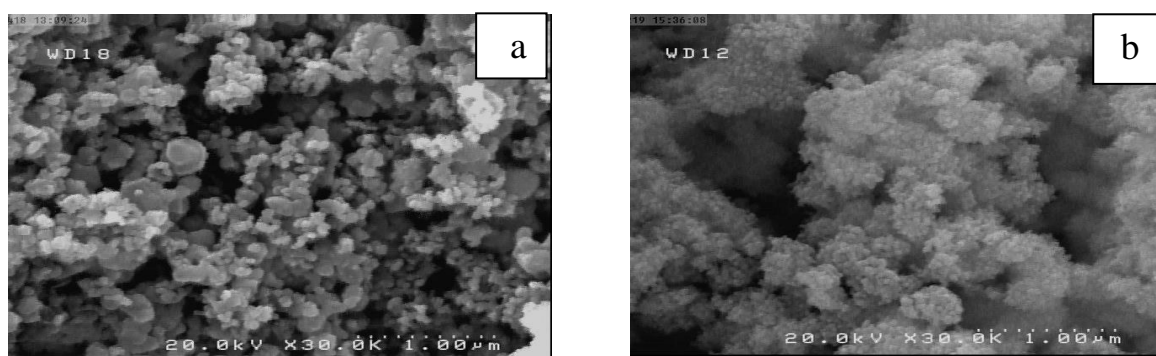


Fig. 1. SEM images of GFO: a) before adsorption b) after adsorption



Fig. 2. The FTIR spectra for GFO

To determine the point of zero charge (pHpzc), 75mg of the adsorbent was exposed to 25ml of 0.01M NaCl under different initial pH values (2, 4, 6, 8, 10, and 12). The pH of the solution was adjusted by adding 0.1M HCl and NaOH.

Furthermore, the solutions were poured into Erlenmeyer flasks, then to be placed on a shaking incubator (JalTajhiz, Iran) at 200rpm and 25°C for 24h. Moreover, the final pH of each solution was measured (WTW model pH7110) and the final pH

(y-axis) versus initial pH (x-axis) was plotted. The point where initial pH is the same as the final pH is known as pH_{pzc}, which in this study was equal to 5.8. Fig.3 shows the pH_{pzc} graph.

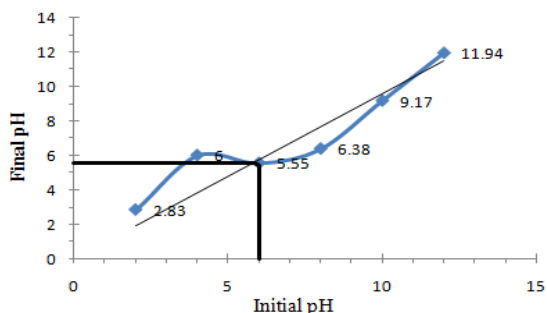


Fig. 3. The pH_{pzc} graph

Table 3 demonstrates the experimental results of CCD for arsenite adsorption on GFO. The response plots were obtained by Design Expert 7 software. Analysis of variance (ANOVA) was used for graphical analysis of data to obtain the interaction between the process variables and the responses. The quality of the polynomial model was assessed by correlation

coefficient (R^2) and its statistical significance was shown through the F-test. The expressions of the model were evaluated with a P-value at a confidence level of 95%. Considering the highest value of R^2 and the absence of any fitting whatsoever, the software selected the 2FI model as the best-fitted model (Table 3). In this study, the goodness of fit %CV turned out to be 10.78. The 2FI (two-factor interaction) model with regression confidences is presented in Eq. 2.

$$R_1 = +38.66 + 0.99 X_1 + 7.34 X_2 - 1.37 X_3 - 0.75 X_4 + 5.99 X_1 X_2 + 4.00 X_1 X_3 - 2.24 X_1 X_4 - 1.26 X_2 X_3 + 0.24 X_2 X_4 + 4.15 X_3 X_4 \quad (2)$$

The quality of the polynomial model was determined by considering the correlation coefficient (R^2) and adjusted R^2 . Table 4 demonstrates the correlation between R^2 and adjusted R^2 in ANOVA analysis. The target is a high amount for R^2 (the closer to 1.00, the better the fit) and a reasonable agreement among R^2 and adjusted R^2 . The R^2 for Arsenic (III) removal was 0.887, indicating a high correlation between independent variables and responses.

Table 3. The ANOVA table and statistical model for Arsenic (III) removal efficiency by GFO

Source	Sum of Squares	df	Mean Square	F Value	p-value	Prob> F
Model	2610.027	10	261.0027	15.02251	< 0.0001	significant
A-Time	23.4235	1	23.4235	1.348185	0.2600	
B-Dose	1291.694	1	1291.694	74.34591	< 0.0001	
C-Concentration	44.854	1	44.854	2.581659	0.1246	
D-pH	13.485	1	13.485	0.776155	0.3893	
AB	574.6808	1	574.6808	33.07686	< 0.0001	
AC	256.5603	1	256.5603	14.76682	0.0011	
AD	80.05776	1	80.05776	4.607879	0.0449	
BC	49.38576	1	49.38576	2.842492	0.1082	
BD	0.907256	1	0.907256	0.052219	0.8217	
CD	274.9793	1	274.9793	15.82696	0.0008	
Residual	330.108	19	17.3741			
Lack of Fit	286.0168	14	20.42977	2.316763	0.1808	not significant
Pure Error	44.0912	5	8.81824			
Cor Total	2940.135	29				

Significant at $p \leq 0.05$

Table 4. Regression analysis for Arsenic (III) removal by GFO, two factor interaction model (2FI)

Regression coefficient type	Arsenic (III) removal (%)
C.V. %	10.78
R-Squared	0.887
Adj R-Squared	0.828
Pred R-Squared	0.634

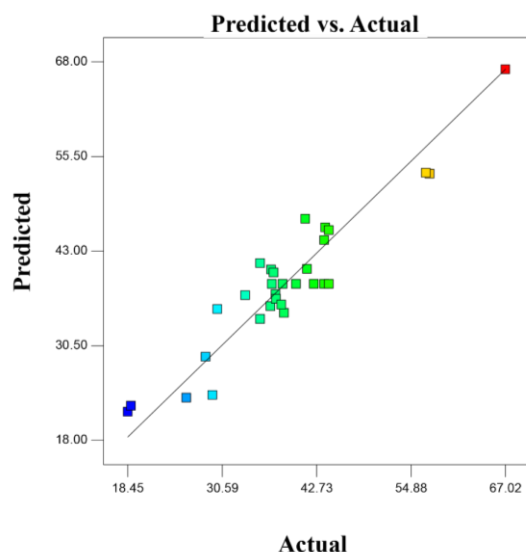


Fig. 4. The relation among predicted and actual results of Arsenic (III) removal efficiency

Fig. 4 illustrates the predicted results versus actual results of Arsenic (III) removal efficiency by GFO, showing a good relation between them in case of Arsenic (III) removal.

To determine the adsorption efficiency of arsenite removal from water over interactive variables, the 3D surface plot was used. Figs. 5-6 display the effect of contact time, adsorbent dosage, initial concentration, and pH on Arsenic (III) removal efficiency.

Fig. 5 shows the contact time and GFO dose on Arsenic (III) removal efficiency. According to this figure, Arsenic (III) removal efficiency was 30.76% to 48.53%. It was increased, once the adsorbent dose rose from 6 to 8g/l and the contact time dropped from 50 to 20.

According to Fig. 5, the increase in contact time reduced the arsenite removal efficiency. Roy et al. (2017) investigated the arsenite removal efficiency at the initial concentration of 100µg/l at a contact time of 10–30 min. They found that removal efficiency rapidly increased until 20 min, then to decrease. Furthermore, both Anjum (2011) and Bang et al.(Bang et al., 2011) discovered that an increase in contact time would enhance removal efficiency of pollutants, which then decline after a certain contact time.

Fast removal in the first stage is due to the

a large number of active sites on the adsorbent surfaces, but with a lapse of time, the remained unoccupied active sites are a result of repulsive force among the arsenic on the adsorbent and bulk phases (Palas Roy et al., 2017; P Roy, Mondal, & Das, 2014).

Reduction of removal efficiency by increasing the contact time in the current study is probably due to the fact that the maximum removal happened in the first 20 min, after which it would decrease.

Based on the results, removal efficiency of arsenite was enhanced by increasing adsorbent dosage (Fig.5). The experimental conditions, studied by Pravin et al. (2009) and Nemade, Kadam, & Shankar (2009) included adsorbent dosage, ranging from 5 to 25g/l at pH=7.2, and an initial arsenite concentration of 1mg/l. They realized that as the adsorbent dosage increased, the removal efficiency was enhanced; therefore, the adsorbent dosage of 25g/l was selected as optimum dosage. Additionally, the results are in good compliance with those of previous studies (Palas Roy et al., 2017; P Roy et al., 2014).

Enhancing the removal efficiency by increasing adsorbent dosage is because of an increase in the surface area of adsorbent and more available active sites for ions to attract (Palas Roy et al., 2017).

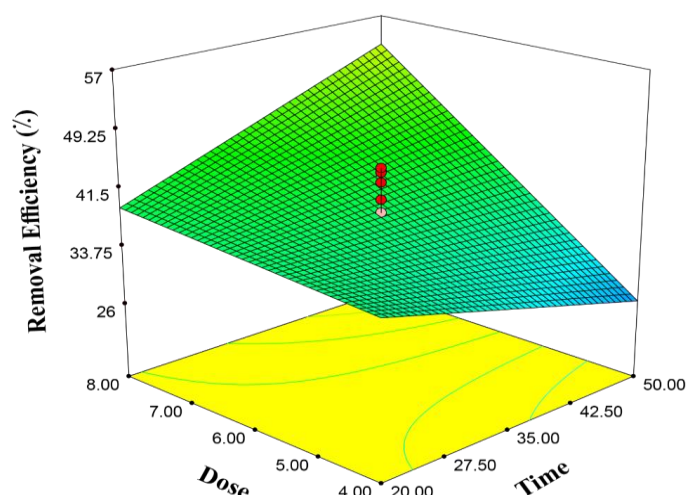


Fig. 5. 3D plot of the GFO dosage and contact time effect on Arsenic (III) removal efficiency (pH= 7, As (III)= 50ppm)

Fig. 6 illustrates the initial concentration of Arsenic (III) and pH impacts on Arsenic (III) removal efficiency as a three-dimensional plot. As it can be seen in Fig.6, the removal efficiency was decreased by increasing the pH and initial concentration of arsenic. Moreover, at a pH of 5.8 and Arsenic (III) concentration of 40 ppm, the arsenic removal efficiency turned out to be 41.9%.

Removal of arsenic from water highly depends on pH (Pillewan et al., 2011). The pH and initial concentration of arsenite ions variations at adsorbent dosage 6g/l and contact time 35min are indicated in Fig.6. The results reveal that arsenite removal efficiency improved up to pH value of 5.8, only to decline at higher pH values. Generally, the ion species in a solution are determined through pH and dissociation constants (C. Wang et al., 2014). The dependence of arsenic species on pH is demonstrated in Eq. 3-4 (Jang M, ChenW, Zou J, Cannon F.s, & Dempsey B, 2010):



However, in acidic pH up to 9, H_3AsO_3^0 is the predominant species. At pH values below 6, there is only H_3AsO_3 , with

H_3AsO_3^0 associated with the amount of H_2AsO_3^- and $\text{H}_2\text{AsO}_3^{2-}$ in pH values of 6-9. These species are increased as the pH value rises (Tajernia, Ebadi, Nasernejad, & Ghafari, 2014).

The pH_{pzc} for GFO was determined at 5.8. When the pH is lower than pH_{pzc}, the surface charge is usually positive. Also, at pH values, higher than pH_{pzc}, a negative charge is generated on the surface (Boddu, Abburi, Talbott, Smith, & Haasch, 2008; Tajernia et al., 2014; Anjum et al., 2011; Nemade et al., 2009; Palas Roy et al., 2017; P Roy et al., 2014). (Hence, the adsorption mechanism of arsenite is divided into two processes: surface complex (pH < 9.1) and electrostatic interactions (pH > 9.1) (Anjum et al., 2011; Nemade et al., 2009).

Based on this figure, the removal efficiency declines by increasing the initial concentration. Nadali et al. (2016) found that in arsenic concentrations of 1-2mg/l, an increase in initial concentration reduced the removal efficiency, a conclusion in good agreement with previous investigations (Mondal, Majumder, & Mohanty, 2008).

Furthermore, Dhiman et al. (2017) observed that in arsenite removal by one-pot synthesized bioceramic buttressed manganese doped iron oxide nanoplateform,

the removal efficiency decreased by increasing the initial concentration.

The decrease in removal efficiency at higher initial concentrations may be due to saturation and reduction of active sites on the adsorbent surfaces for higher amounts of arsenic adsorption (P Roy et al., 2014).

Design-Expert software represents an equation with the highest Arsenic (III) removal efficiency, the lowest adsorbent dosage, and contact time. Table 5 illustrates the appropriate conditions for optimal operation, showing the optimal

predicted removal efficiency (equal to 66.99%) was achieved when the initial concentration of Arsenic (III) was 30ppm, for an operating time of 49.9 min, GFO dosage of 8g/l, and pH=5. Under these conditions, GFO can trigger the arsenite concentration to reach global arsenic standards. A laboratory experiment was conducted to approve the validity of the predicted optimum condition by CCD. As can be seen in Table 5, the result of the experiment was in good agreement with the predicted optimized condition.

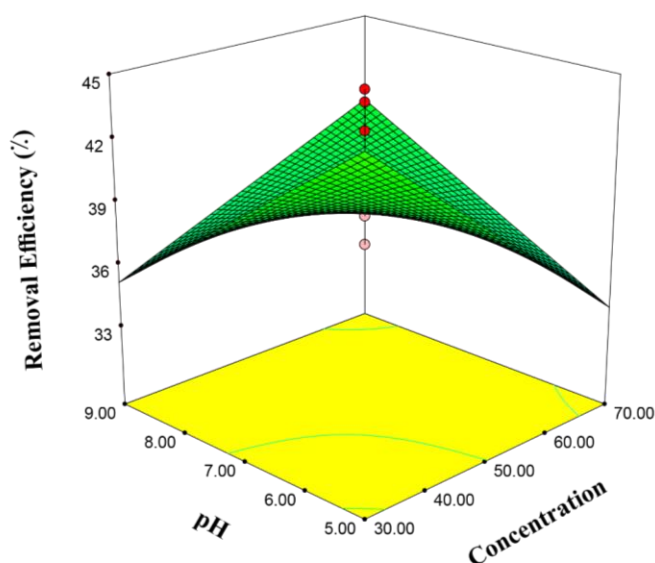


Fig. 6. 3D plot of the effect of initial concentration of arsenic (III) and pH on Arsenic (III) removal efficiency (GFO= 6g/l, time= 35min)

Table 5. Optimization of central composite with RSM

Name	Goal	Lower Limit	Upper Limit	Lower Weight	Upper Weight	Importance
Time	is in range	20	50	1	1	3
Dose	is in range	4	8	1	1	3
Concentration	is in range	30	70	1	1	3
pH	is in range	5	9	1	1	3
As(III) removal eff.	Maximize	18.45	67.02	1	1	3
Number	Time	Dose	Concentration	pH	As (III) rem. eff. (%)	Desirability
Validation experiment at optimized process condition	49.99	8	30	5	66.99547	0.999495
RSM predictions	49.99	8	30	5	67	

CONCLUSIONS

In the present study, the arsenite ion was removed from the aqueous solution by synthesized GFO. The RSM method, based on CCD, was used to select a suitable model and optimized the process. The values of the regression coefficient (R^2) and adjusted

regression coefficient (Adj. R^2) for arsenite removal were 0.88 and 0.82, respectively. These coefficient values were close to one another. Moreover, the predicted regression coefficient (Pred. R^2) of the model was 0.63, indicating that the empirically-obtained values were highly consistent with the

predicted values by the model. By increasing the GFO dosage, the removal efficiency improved. In addition, reducing the contact time, pH, and initial concentration of arsenite had a negative impact on arsenite removal efficiency. According to Design-Expert software, the optimum conditions for arsenite removal by GFO were as follows: adsorbent dose = 8g/l, contact time = 49.9min, initial arsenite concentration = 30ppm, and pH = 5. At optimized conditions, the arsenite removal efficiency was 66.99% with a desirability of 0.99. Iron Oxide Granules remained soluble Iron and color in water. However, conventional water treatment plants can remove this residual Iron and color. Hence, it is suggested that this unit be placed before activated carbon or sand filter unit in water treatment plants. The advantages of this adsorbent are its easy manufacturing, easy operation, and proper removal of arsenite. Nevertheless, there is a big disadvantage for this method, which is the high adsorbent consumption for arsenite. For future studies, it is recommended to investigate the hybrid method of this adsorbent with suitable beds for arsenite removal. Additionally, it is suggested to examine the adsorbents after the usage for hazardousness by the TCLP test.

ACKNOWLEDGEMENTS

This work is part of a master's thesis. The authors would like to thank Qom University of medical sciences for its financial support of this research. They also wish to thank the staff of the Environmental Health Engineering lab for their cooperation and assistance.

GRANT SUPPORT DETAILS

The present research has been financially supported by Qom University of Medical Sciences (grant No.96822).

CONFLICT OF INTEREST

The authors declare that there is no conflict of interests, regarding the publication of this manuscript. In addition, the ethical

issues, including plagiarism, informed consent, misconduct, data fabrication, and/or falsification, double publication and/or submission, and redundancy has been completely observed by the authors.

LIFE SCIENCE REPORTING

No life science threat was practiced in this research.

REFERENCES

- AlOmar, M. K., Alsaadi, M. A., Hayyan, M., Akib, S. and Hashim, M. A. (2016). Functionalization of CNTs surface with phosphonium based deep eutectic solvents for arsenic removal from water. *Applied Surface Science.*, 389, 216-226.
- Andrew, D., Eugene, W. R. and Lenore, S. (2005). *Standard methods for the examination of water and wastewater (Vol. 1)*. American Public Health Association).
- Anjum, A., Lokeswari, P., Kaur, M. and Datta, M. (2011). Removal of As (III) from aqueous solutions using montmorillonite. *Journal of Analytical Sciences, Methods and Instrumentation.*, 1(02), 25.
- Bang, S., Pena, M. E., Patel, M., Lippincott, L., Meng, X. and Kim, K.W. (2011). Removal of arsenate from water by adsorbents: a comparative case study. *Environmental geochemistry and health.*, 33(1), 133-141.
- Barati, A. H., Maleki, A. and Alasvand, M. (2010). Multi-trace elements level in drinking water and the prevalence of multi-chronic arsenical poisoning in residents in the west area of Iran. *Science of the Total Environment.*, 408, 1523-1529.
- Bhandari, N., Reeder, R. J. and Strongin, D. R. (2012). Photoinduced oxidation of arsenite to arsenate in the presence of goethite. *Environmental science & technology.*, 46(15), 8044-8051.
- Boddu, V. M., Abburi, K., Talbott, J. L., Smith, E. D. and Haasch, R. (2008). Removal of arsenic (III) and arsenic (V) from aqueous medium using chitosan-coated biosorbent. *Water Research.*, 42(3), 633-642.
- Bringas, E., Saiz, J. and Ortiz, I. (2015). Removal of As (V) from groundwater using functionalized magnetic adsorbent materials: effects of competing ions. *Separation and Purification Technology.*, 156, 699-707.
- Chang, Q., Lin, W. and Ying, W.c. (2010). Preparation of iron-impregnated granular activated carbon for arsenic removal from drinking water. *Journal of Hazardous Materials.*, 184(1-3), 515-522.

- Cheng, Z., Fu, F., Dionysiou, D. D. and Tang, B. (2016). Adsorption, oxidation, and reduction behavior of arsenic in the removal of aqueous As(III) by mesoporous Fe/Al bimetallic particles. *Water Research.*, 96, 22-31.
- Cornell, R. M. and Schwertmann, U. (2003). *The iron oxides: structure, properties, reactions, occurrences and uses.* (John Wiley & Sons).
- Dhiman, N., Fatima, F., Saxsena, P. N., Roy, S., Rout, P. K. and Patnaik, S. (2017). Predictive modeling and validation of arsenite removal by a one pot synthesized bioceramic buttressed manganese doped iron oxide nanoplatfrom. *RSC Advances.*, 7(52), 32866-32876.
- Guivar, J. A. R., Bustamante D., A., Gonzalez , J. C., A. Sanches , E., Morales, M. A., M. Raez, J. and Arencibia, A. (2018). Adsorption of arsenite and arsenate on binary and ternary magnetic nanocomposites with high iron oxide content. *Applied Surface Science.*, 454, 87-100.
- Gupta, A., Yunus, M. and Sankaramakrishnan, N. (2012). Zerovalent iron encapsulated chitosan nanospheres—A novel adsorbent for the removal of total inorganic Arsenic from aqueous systems. *Chemosphere.*, 86(2), 150-155.
- Jang M, ChenW, Zou J, Cannon F.s and Dempsey B. (2010). Arsenic Removal by Iron-Modified Activated Carbon: WERC, a Consortium for Environmental Education and Technology Development at New Mexico State University.
- Jian, M., Liu, B., Zhang, G., Liu, R. and Zhang, X. (2015). Adsorptive removal of arsenic from aqueous solution by zeolitic imidazolate framework-8 (ZIF-8) nanoparticles. *Colloids and Surfaces A: Physicochemical and Engineering Aspects.*, 465, 67-76.
- Kabay, N., Bundschuh, J., Hendry, B., Bryjak, M., Yoshizuka, K., Bhattacharya, P. and Anac, S. (2010). *The global arsenic problem: challenges for safe water production:* CRC press.
- Lata, S. and Samadder, S. (2016). Removal of arsenic from water using nano adsorbents and challenges: a review. *Journal of environmental management.*, 166, 387-406.
- Lee, T. Z. E., Krongchai, C., Lu, N. A. L. M. I., Kittiwachana, S. and Sim, S. F. (2015). Application of central composite design for optimization of the removal of humic substances using coconut copra. *International Journal of Industrial Chemistry.*, 6(3), 185-191.
- Litter, M. I., Morgada, M. E. and Bundschuh, J. (2010). Possible treatments for arsenic removal in Latin American waters for human consumption. *Environmental Pollution.*, 158(5), 1105-1118.
- Malakootian, M., Mahdizadeh, H., Nasiri, A., Mirzaenia, F., Hajhoseini, M. and Amirmahani, N. (2018). Investigation of the efficiency of microbial desalination cell in removal of arsenic from aqueous solutions. *Desalination.*, 438, 19-23.
- Mao, K., Zhang, H., Wang, Z., Cao, H., Zhang, K., Li, X. and Yang, Z. (2019). Nanomaterial-based aptamer sensors for arsenic detection. *Biosensors and Bioelectronics.*, 111785.
- Mondal, P., Majumder, C. and Mohanty, B. (2008). Effects of adsorbent dose, its particle size and initial arsenic concentration on the removal of arsenic, iron and manganese from simulated ground water by Fe³⁺ impregnated activated carbon. *Journal of Hazardous Materials.*, 150(3), 695-702.
- Mostafaloo, R., Mahmoudian, M. H. and Asadi-Ghalhari, M. (2019). BiFeO₃/Magnetic Nanocomposites for the Photocatalytic Degradation of Cefixime From Aqueous Solutions under Visible Light. *Journal of Photochemistry and Photobiology A: Chemistry.*, 111926.
- Nadali, A., Khoobi, M., Nabizadeh, R., Naseri, S. and Mahvi, A. H. (2016). Performance evaluation of montmorillonite and modified montmorillonite by polyethyleneimine in removing arsenic from water resources. *Desalination and Water Treatment.*, 57(45), 21645-21653.
- Nasir , A. M., Goh, P. S. and Ismail, A. F. (2018). Novel synergistic hydrous iron-nickel-manganese (HINM) trimetal oxide for hazardous arsenite removal. *Chemosphere.*, 200, 504-5012.
- Nemade, P. D., Kadam, A. and Shankar, H. (2009). Adsorption of arsenic from aqueous solution on naturally available red soil. *Journal of Environmental Biology.*, 30(9), 499-504.
- Ociński, D., Jacukowicz-Sobala, I., Mazur, P., Raczyk, J. and Kociolek-Balawejder, E. (2016). Water treatment residuals containing iron and manganese oxides for arsenic removal from water—Characterization of physicochemical properties and adsorption studies. *Chemical Engineering Journal.*, 294, 210-221.
- Pillewan, P., Mukherjee, S., Roychowdhury, T., Das, S., Bansawal, A. and Rayalu, S. (2011). Removal of As (III) and As (V) from water by copper oxide incorporated mesoporous alumina. *Journal of Hazardous Materials.*, 186(1), 367-375.
- Ristić, M., De Grave, E., Musić, S., Popović, S. and Orehovec, Z. (2007). Transformation of low crystalline ferrihydrite to α -Fe₂O₃ in the solid state. *Journal of molecular structure.*, 834, 454-460.

Roy, P., Dey, U., Chattoraj, S., Mukhopadhyay, D. and Mondal, N. K. (2017). Modeling of the adsorptive removal of arsenic (III) using plant biomass: a bioremedial approach. *Applied Water Science.*, 7(3), 1307-1321.

Roy, P., Mondal, N. and Das, K. (2014). Modeling of the adsorptive removal of arsenic :a statistical approach. *Journal of Environmental Chemical Engineering.*, 2(1), 585-597.

Salameh, Y., B. Albadarin, A., Allen, S., Walker , G. and Ahmad, M. N. M. (2015). Arsenic(III,V) adsorption onto charred dolomite: Charring optimization and batch studies. *Chemical Engineering Journal.*, 259, 663-671.

Tajernia, H., Ebadi, T., Nasernejad, B. and Ghafari, M. (2014). Arsenic removal from water by sugarcane bagasse: an application of response surface methodology (RSM). *Water, Air, & Soil Pollution.*, 225(7), 2028.

Usefi, S. and Asadi-Ghalhari, M. (2019). Modeling and Optimization of the Coagulation–Flocculation Process in Turbidity Removal from Aqueous Solutions Using Rice Starch. *Pollution.*, 5(3), 623-636.

Wang, C., Luo, H., Zhang, Z., Wu, Y., Zhang, J. and Chen, S. (2014). Removal of As (III) and As (V) from aqueous solutions using nanoscale zero valent iron-reduced graphite oxide modified composites. *Journal of Hazardous Materials.*, 268, 124-131.

Wang, J., Wei, Y., Zhang, J., Ji, L., Huang, Y. and Chen, Z. (2014). Synthesis of pure-phase BiFeO₃ nanopowder by nitric acid-assisted gel. *Materials Letters.*, 124, 242-244.

Wang, J., Xu , W., Chen, L., Huang, X. and Liu, J. (2014). Preparation and evaluation of magnetic nanoparticles impregnated chitosan beads for arsenic removal from water *Chemical Engineering Journal.*, 251, 25-34.

